Developmental Biology 454 (2019) 85–95

Contents lists available at ScienceDirect

Developmental Biology

journal homepage: www.elsevier.com/locate/developmentalbiology

# Blood feeding activates the vitellogenic stage of oogenesis in the mosquito *Aedes aegypti* through inhibition of glycogen synthase kinase 3 by the insulin and TOR pathways

Luca Valzania, Melissa T. Mattee [1], Michael R. Strand, Mark R. Brown [*]

*Department of Entomology, University of Georgia, Athens, GA, 30602, USA*

ARTICLE INFO

*Keywords:*
Insect
Hematophagy
Reproduction
Egg
Hormone
Signaling

ABSTRACT

Most mosquitoes, including *Aedes aegypti,* only produce eggs after blood feeding on a vertebrate host. Oogenesis in *A. aegypti* consists of a pre-vitellogenic stage before blood feeding and a vitellogenic stage after blood feeding. Primary egg chambers remain developmentally arrested during the pre-vitellogenic stage but complete oogenesis to form mature eggs during the vitellogenic stage. In contrast, the signaling factors that maintain primary egg chambers in pre-vitellogenic arrest or that activate vitellogenic growth are largely unclear. Prior studies showed that *A. aegypti* females release insulin-like peptide 3 (ILP3) and ovary ecdysteroidogenic hormone (OEH) from brain neurosecretory cells after blood feeding. Here, we report that primary egg chambers exit pre-vitellogenic arrest by 8 h post-blood meal as evidenced by proliferation of follicle cells, endoreplication of nurse cells, and formation of cytoophidia. Ex vivo assays showed that ILP3 and OEH stimulate primary egg chambers to exit pre-vitellogenic arrest in the presence of nutrients but not in their absence. Characterization of associated pathways indicated that activation of insulin/insulin growth factor signaling (IIS) by ILP3 or OEH inactivated glycogen synthase kinase 3 (GSK3) via phosphorylation by phosphorylated Akt. GSK3 inactivation correlated with accumulation of the basic helix-loop-helix transcription factor Max and primary egg chambers exiting pre-vitellogenic arrest. Direct inhibition of GSK3 by CHIR-99021 also stimulated Myc/Max accumulation and primary egg chambers exiting pre-vitellogenic arrest. Collectively, our results identify GSK3 as a key factor in regulating the pre- and vitellogenic stages of oogenesis in *A. aegypti.*

## 1. Introduction

Germ cells in the ovaries of female animals produce oocytes that become eggs through the process of oogenesis (Gu et al., 2015). In vertebrates, hormonal signals integrate seasonal and nutritional cues to promote or delay oogenesis (Lucy, 2011; Clarke and Arbabi, 2016; Ikegami and Yoshimura, 2016). This begins with the release of gonadotropin releasing hormone (GnRH) that functions as a central signal in activating oogenesis by stimulating the release of other hormones (Zhang and Liu, 2015). Among invertebrates, oogenesis has been most studied in *Drosophila melanogaster*, which is an insect in the order Diptera (flies). The paired ovaries of *D. melanogaster* are divided into multiple ovarioles that continuously produce eggs when females feed on protein-rich diets (Lee, 2015). Germ cells in the germaria of proximal ovarioles divide asymmetrically to self-renew and form cystoblasts (Drummond-Barbosa and Spradling, 2001). In turn, each cystoblast divides mitotically with incomplete cytokinesis to produce one oocyte and fifteen nurse cells that form an egg chamber (= follicle) when enveloped by somatic follicle cells. Egg chambers then sequentially progress through oogenesis by growing and packaging yolk (vitellogenesis) to form mature eggs that females fertilize and lay (Bastock and St Johnston, 2008). No centrally released factor like GnRH activates oogenesis in *D. melanogaster*, but several other hormones including insulin-like peptides (ILPs), the sesquiterpenoid juvenile hormone (JH), and steroid hormone ecdysone have key regulatory functions (LaFever and Drummond-Barbosa, 2005; LaFever et al., 2010; Gancz and Gilboa, 2013; Hartman et al., 2013; Huang and Kalderon, 2014; Burn et al., 2015; Laws and Drummond-Barbosa, 2016; Meiselman et al., 2017; Armstrong and Drummond-Barbosa, 2018).

Mosquitoes are also in the order Diptera but reproductively differ

* Corresponding author.
*E-mail address:* mrbrown@uga.edu (M.R. Brown).
[1] Present address: South Fulton Extension Office, 1757 Washington Road, East Point, GA 30344-4151.

https://doi.org/10.1016/j.ydbio.2019.05.011
Received 23 April 2019; Received in revised form 21 May 2019; Accepted 22 May 2019
Available online 30 May 2019

from *D. melanogaster* in that most species only produce eggs after feeding on blood from a vertebrate host. This requirement also results in females cyclically producing eggs and underlies why a number of mosquitoes are capable of acquiring and transmitting pathogens that cause vertebrate disease (Clements, 1992). Oogenesis in mosquitoes has been most studied in *Aedes aegypti,* which is the primary vector of the viruses that cause Dengue fever, yellow fever and Zika syndrome in humans (Roy et al., 2016; Strand et al., 2016; Zhu and Noriega, 2016). Oogenesis in *A. aegypti* consists of a pre-vitellogenic stage that occurs before blood feeding and a vitellogenic stage that occurs after blood feeding (Laurence, 1977; Clements, 1992). The paired ovaries of *A. aegypti* are subdivided into 50–60 ovarioles. The pre-vitellogenic stage begins in the late pupal stage when self-renewing germ cells produce cystoblasts. Individual cystoblasts in each ovariole then divide with incomplete cytokinesis to form one oocyte and seven nurse cells that are enveloped by somatic follicle cells to form a primary egg chamber (Fig. 1). In the first two days after emergence as an adult, each primary egg chamber approximately doubles in size in response to JH III that is released from the corpora allata (Laurence and Simpson, 1974; Gwadz and Spielman, 1973; Hagedorn et al., 1977; Hernández-Martínez et al., 2007, 2016). Primary egg chambers thereafter enter an arrest phase that indefinitely persists unless a female blood feeds, which stimulates the vitellogenic stage of oogenesis. During the vitellogenic stage, the primary egg chamber in each ovariole develops into a mature egg, while secondary egg chambers consisting of an oocyte, nurse cells and surrounding follicle cells form proximally to each primary egg chamber (Laurence, 1977) (Fig. 1).

Blood feeding stimulates neurosecretory cells in the brain to release ILPs and a second peptidyl hormone named ovary ecdysteroidogenic hormone (OEH) (Brown et al., 1998, 2008; Strand et al., 2016). Among the eight ILPs that *A. aegypti* encodes, ILP3 binds with high affinity to the insulin receptor (IR), a type of receptor tyrosine kinase (RTK), while OEH binds to a related RTK named the OEH receptor (OEHR) (Brown et al., 2008; Wen et al., 2010; Vogel et al., 2015). Both receptors are expressed by follicle cells of primary egg chambers (Riehle et al., 2002; Vogel et al., 2015). While ILP3 and OEH bind different receptors, both activate insulin/insulin growth factor signaling (IIS), which induces follicle cells to produce ecdysone (Dhara et al., 2013; Vogel et al., 2015). Ecdysone is converted to 20-hydroxyecdysone (20E), which together with increased amino acids from blood feeding, JH III, and activation of the IIS and TOR pathways regulate yolk production by the fat body (Gulia-Nuss et al., 2011; Hansen et al., 2014; Roy et al., 2015; Roy et al., 2016). Primary egg chambers complete oogenesis by packaging yolk from the fat body and RNA and proteins from nurse cells that degenerate. Follicle cells then secrete an egg shell (chorion) before also degenerating, which results in formation of a mature egg. Females fertilize and lay 80–120 mature eggs as a single clutch. Secondary egg chambers then become primary egg chambers that enter pre-vitellogenic arrest until a female consumes a second blood meal (Fig. 1).

Unclear from previous studies are the factors that maintain primary egg chambers in pre-vitellogenic arrest in non-blood fed (NBF) females or that induce the vitellogenic stage after a blood meal. In this study we assessed whether increased nutrients alone stimulate primary egg chambers in *A. aegypti* to exit pre-vitellogenic arrest versus the alternative hypothesis that specific endocrine factors produced in response to blood feeding are required. We report that primary egg chambers begin to exit pre-vitellogenic arrest within 2 h of a female blood feeding, while ex vivo assays indicate that primary egg chambers exit pre-vitellogenic arrest in direct response to ILP3 and OEH plus increased nutrients. Our results further suggest blood feeding activates the vitellogenic stage of oogenesis through inhibition of glycogen synthase kinase 3 (GSK3) by the insulin and TOR pathways.

## 2. Materials and methods

### 2.1. Mosquitoes

The University of Georgia strain of *A. aegypti* named UGAL was reared as previously described (Gulia-Nuss et al., 2015). Handling and anesthetization of rats for blood feeding females followed the protocol (A2018 02-002-R2) approved by The University of Georgia Institutional Animal Care and Use Committee, which oversees and provides veterinary care, maintains an Assurance of Compliance with the US Public Health Service and is accredited by the Association for Assessment and Accreditation of Laboratory Animal Care International and licensed by the US Department of Agriculture.

### 2.2. Reagents

Bioactive ILP3 was produced by chemically synthesizing the A and B chains using standard Fmoc chemistry followed by formation of the correct interchain disulfide bonds as previously reported (Brown et al., 2008). Recombinant OEH was produced in *Escherichia coli* and purified

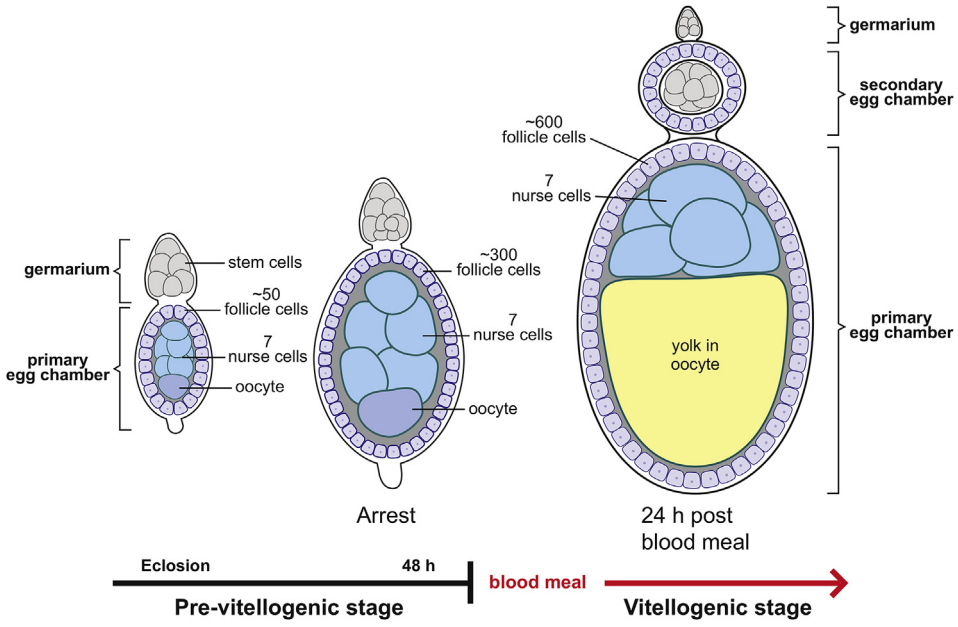


**Fig. 1.** Schematic illustrating the pre-vitellogenic (left panel) and vitellogenic stages (right panel) of oogenesis in *Aedes aegypti*.

by HPLC (Wen et al., 2010; Gulia-Nuss et al., 2015; Vogel et al., 2015). Stock solutions of 20E and JH III (Sigma) were solubilized in ethanol. OSI-906 (LC Laboratories, Woburn, MA), Torin 2 (Cayman, Ann Arbor, MI), and CHIR-99021 (Selleck Chemicals, Houston, TX) prepared in dimethyl sulfoxide (DMSO) were diluted in Sf-900 II serum free medium (= Sf900, Gibco) or buffered saline to contain 0.8% or less DMSO.

### 2.3. 5-Ethynyl-2′-deoxyuridine, phospho-histone H3, and cytoophidia labeling

Adult females (3–5 days old) were starved for 4 h followed by feeding a 10% sugar solution containing 10 mM of the nucleotide analog 5-ethynyl-2′-deoxyuridine (EdU) (Sigma 900584) for 2 h. These sugar fed females were then blood fed 6–7 h later. Only females that blood fed to repletion (i.e. consumed a full blood meal) were used to collect ovaries at specific times post blood meal (PBM). Ovaries were collected by removing them from females in phosphate buffered saline (PBS) using forceps. Samples were fixed in 4% paraformaldehyde in PBS for 20 min at room temperature (RT). Samples were then permeabilized with 0.3% Triton X100 in PBS (PBT) for 1 h and processed for EdU labeling at 4 °C using the Click-iT® EdU Alexa Fluor 488 Imaging Kit (C10337, ThermoFisher). Ovaries were then transferred to a glycerol/PBS drop on a microscope slide, disrupted with forceps to separate ovarioles, and sealed with a cover slip. For phospho-histone H3 (pHH3) and cytoophidia/cytidine 5′-triphosphate synthase (CTPsyn) labeling, ovaries were dissected from NBF or blood-fed females at different times, followed by fixation and permeabilization as described above. After rinsing in PBT, samples were preincubated in 5% goat serum and 0.3% Triton X100 in PBS (GS-PBT) for 10 min at RT, followed by addition of pHH3 (Ser 10) antibody (1:1000 dilution; sc-8656-R Santa Cruz Biotechnology) or CTPsyn antibody (1:100; 15914-1-AP Proteintech) and incubation overnight at 4 °C. After rinsing, ovaries were incubated with goat-anti-rabbit antibody-AlexaFluor 488 (1:1000; A11070 Molecular Probes) in GS-PBT at RT for 2 h. Rinsed ovaries were then slide mounted and examined using a Zeiss LSM 710 confocal microscope. The number of EdU or anti-pHH3 labeled nuclei in follicle cells in primary egg chambers were counted by capturing optical sections from the surface to the middle of each chamber (i.e. the total number of follicle cells per half an egg chamber were analyzed for each sample). Primary egg chamber circumference and nuclear diameter of EdU-labeled cells were determined using ImageJ software.

### 2.4. Ex vivo assays

Ovaries from NBF females were collected and cultured as two ovary pairs in 60 µl total of buffered saline or Sf900 per 0.6 ml microtube cap. ILP3 (0.3 µM), OEH (0.3 µM), 20E (17 µM), or JH III (17 µM) alone or with EdU (10 mM; added in 10 µl) was added to 50 µl of each primary culture. After incubation for 6 h at 27 °C, ovaries were processed for pHH3 or EdU staining as above, after which cell counts and egg chamber measurements were made as above. For inhibitor assays, triplicate sets of ovaries in Sf900 were incubated for 15 min with OSI-906 or Torin2 at different concentrations prior to adding ILP3 (0.3µM) or OEH (1.7µM) alone or with EdU. CHIR-99021 (200 µM) was added to triplicate sets of ovaries from NBF females at the same time as ILP3 plus EdU. Ovaries treated with ILP3 or OEH alone with or without DMSO served as positive controls, while ovaries in Sf900 or saline alone served as negative controls. Forty primary egg chambers from nine independently acquired and treated ovary pairs were examined across all treatments in Sf900 while nine primary egg chambers from nine independently acquired and treated ovary pairs were examined across all treatments in saline.

### 2.5. Immunoblotting

Ovaries from NBF and females that blood fed to repletion were incubated alone or with hormones and inhibitors in buffered saline or Sf900 for 30 min or 6 h, as above in triplicate, and then transferred and pooled in 30 µl of PRO-PREP protein extraction solution (17081 Intron Biotechnology) with 1X protease and phosphatase inhibitors (78443 ThermoFisher Scientific). Samples were extracted by homogenization with a motorized pellet pestle on ice, centrifuged (3 min at 10000 rpm, 4 °C), and stored at −80 °C. The protein concentration of the supernatant was measured using Coomassie Plus Protein Assay Reagent (1856210 ThermoFisher). Ovary extracts (50 µg of protein per lane) were mixed with 2x sample buffer (161–0737 Bio-Rad) and 5% β-mercaptoethanol (M3148 Sigma Aldrich), boiled for 10 min and loaded onto 4–20% Tris-glycine gels for electrophoresis (456–8094 Bio-Rad). Proteins were transferred to polyvinyl difluoride membranes (88520 ThermoFisher Scientific) at 0.35 A for 1 h at 4 °C. Membranes were blocked with blocking buffer (5% nonfat dry milk in PBS with 0.1% Tween 20) for 1 h at RT and probed with primary antibodies in blocking buffer that recognize *A. aegypti*: CTPsyn (see above), phospho-p70 S6 kinase (pS6K; 1:1000, 9209 Cell Signaling Technology); phospho-adenosine monophosphate-activated protein kinase (pAMPK) (1:1000, 2531 Cell Signaling Technology); phospho-*Drosophila* Akt (pAkt; 1:1000, p-Ser505, 4054 Cell Signaling Technology); phospho-GSK3 (pGSK3; 1:1000, 9331 Cell Signaling Technology), Forkhead box O (FoxO; 1:1000, gift from C. Sim (Sim and Denlinger, 2013)), phospho-FoxO (pFoxO; 1:1000, 9664 Cell Signaling Technology) phospho-p44/42 mitogen-activated protein kinases (MAPK = pERK1/2; 1:1000, 9101 Cell Signaling Technology); phospho-stress-activated kinase/c-Jun N-terminal kinase (pJNK; 1:1000 dilution, 9251 Cell Signaling Technology); phospho-p38 MAPK (pp38; 1:1000, 9211 Cell Signaling Technology) and actin (1:1000, A2103 Sigma) (Valzania et al., 2018). In *A. aegypti, myc* (XP_021694469.1) and max (XP_001662341.2) are single copy genes that encode basic helix-loop-helix transcription factors that are conserved across eukaryotes (Zhang et al., 2013; Gerlach et al., 2017). Sequence analysis in combination with immunoblotting data strongly suggested that a rabbit polyclonal antibody from Novus Biologicals (NB600-336, 1:1000) recognizes *A. aegypti* Myc, while a rabbit polyclonal antibody from LifeSpan BioSciences (LSBio 7667, 1:1000) recognizes *A. aegypti* Max (Fig. S1, Fig. S2).

After primary antibody incubation and washing, all membranes were probed with a horseradish peroxidase labeled goat anti-rabbit secondary antibody (1:5000, 111-035-003 Jackson ImmunoResearch), diluted in blocking buffer for 2 h at room temperature. Immunoreactive protein bands were then visualized after washing using the Clarity Western ECL Substrate (170–5060 Bio-Rad). Immunoblots were directly recorded and digitized using the G:BOX chemiluminescence imaging system (Syngene, Synoptics group). Three immunoblots prepared from triplicate biological samples that were independently acquired were examined for each protein target. For immunoblots that visualized CTPsyn, relative abundance was estimated by densitometry using ImageJ software, which calculated in arbitrary units the density of the CTPsyn and actin loading control bands to generate a CTPsyn/actin ratio for each replicate. Images for all immunoblots were assembled into figures using Adobe Photoshop CS6 and Adobe Illustrator CC 2019.

### 2.6. Above reagents and sources are listed in key resources table

Key resources table.

| Reagent or resource | Source | Identifier |
|---|---|---|
| Antibodies – all polyclonal | | |
| CTP synthase | Proteintech | Cat#15914-1-AP |
| phospho-histone H3 | Santa Cruz Biotechnology | Cat#sc-8656-R |
| phospho-p70 S6 kinase | Cell Signaling Technology (CST) | Cat#9209 |
| phospho-adenosine monophosphate-activated protein kinase | CST | Cat#2531 |
| phospho-*Drosophila* Akt p-Ser505 | CST | Cat#4054 |

(*continued on next page*)

(*continued*)

| Reagent or resource | Source | Identifier |
|---|---|---|
| phospho-GSK3 | CST | Cat#9331 |
| Forkhead box O (FoxO) | Lab of C. Sim | |
| phospho-FoxO | CST | Cat#9664 |
| phospho-p44/42 mitogen-activated protein kinases = pERK1/2 | CST | Cat#9101 |
| phospho-stress-activated kinase/c-Jun N-terminal kinase | CST | Cat#9251 |
| phospho-p38 mitogen-activated protein kinase | CST | Cat#9211 |
| actin | Sigma | Cat#A2103 |
| Myc | Novus Biologicals | Cat#NB600-336 |
| Myc | LifeSpan BioSciences | Cat#LSBio 7667 |
| Chemicals, Peptides, and Recombinant Proteins | | |
| *Aedes aegypti* ILP3 – custom peptide synthesis | CPC Scientific Inc | |
| *Aedes aegypti* OEH – recombinant protein | Brown/Strand lab | |
| OSI-906 | LC Laboratories | Cat#L-5814 |
| Torin 2 | Cayman | Cat#14185 |
| CHIR-99021 | Selleck Chemicals | Cat#CT99021 |
| JH III | Sigma | Cat#J2000 |
| 20-OH ecdysone | Sigma | Cat#H5142 |
| Critical Commercial Assays | | |
| Click-iT® EdU Alexa Fluor 488 Imaging Kit | ThermoFisher | Cat#C10337 |
| Experimental Models: Organisms/Strains | | |
| Yellow fever mosquito, *Aedes aegypti* | Brown/Strand lab | UGAL strain |

### 2.7. Data analysis

Microsoft Excel 2010 was used for data organization while statistical analyses were conducted using either JMP (SAS, Cary, NC) or GraphPad Prism 7.0 which were also used for generating figures.

## 3. Results

### 3.1. Primary egg chambers enter the vitellogenic stage of oogenesis within 8 h of blood feeding

We measured several parameters to assess when primary egg chambers exit pre-vitellogenic arrest after *A. aegypti* females blood feed (Fig. 1). No differences were detected in the circumference or number of follicle cells per primary egg chamber up to 8 h PBM, while both measures approximately doubled between 8 and 24 h PBM (Fig. 2A). Feeding the nucleotide analog EdU to NBF females resulted in almost no labeling of follicle and nurse cell nuclei, which indicated that little or no DNA synthesis occurs in primary egg chambers during pre-vitellogenic arrest (Fig. 2B). In contrast, EdU labeling of follicle and nurse cell nuclei visibly increased by 2 h PBM while immunostaining with a pan anti-pHH3 antibody showed that the number of follicle cells undergoing mitosis also rose 2–12 h PBM before declining at 16 and 24 h (Fig. 2B and C). That nurse cell nuclei were labeled by EdU but not anti-pHH3 indicated that nurse cells endoreplicate but do not further divide after primary egg chambers exit pre-vitellogenic arrest. CTPsyn, a key enzyme in the CTP synthesis pathway, forms cytoplasmic filaments (cytoophidia) in replicating cells from diverse organisms (Liu, 2010, 2016). An anti-CTPsyn antibody detected a 73 kDa protein corresponding to the predicted mass of *A. aegypti* CTPsyn (XP_001650904.1) plus a 56 kDa protein that is likely a post-translational cleavage product (Park et al., 2003) (Fig. 2D). Both the 73 and 56 kDa products were more abundant in ovaries at 8 and 24 h PBM than in ovaries from NBF and 2 h PBM females (Fig. 2D). Correspondingly, cytoophidia were present in follicle and nurse cells from 8 to 24 h PBM but were absent in primary egg chambers from NBF and 2 h PBM females (Fig. 2E). We thus concluded that primary egg chambers begin to exit pre-vitellogenic arrest between 2 and 8 h PBM as evidenced by an increase in DNA synthesis and mitosis of follicle cells, endoreplication of nurse cells, and formation of cytoophidia.

### 3.2. ILP3 and OEH induce primary egg chambers to exit pre-vitellogenic arrest

A previously developed ex vivo assay showed that ovaries from NBF females do not produce ecdysone when cultured in saline or Sf900 medium containing amino acids and other nutrients, but adding ILP3 or OEH dose-dependently stimulates ecdysone production (Brown et al., 2008; Gulia Nuss et al., 2011). Ovaries produce more ecdysone in response to these hormones in Sf900 than saline, but adding the TOR pathway inhibitor rapamycin reduces that amount of ecdysone produced in Sf900 to levels in saline, which suggests nutrient sensing also plays a role in ecdysone biosynthesis (Brown et al., 2008; Gulia-Nuss et al., 2011; Dhara et al., 2013). Given these findings, we reasoned that primary egg chambers could exit pre-vitellogenic arrest in response to ILP3, OEH and/or increased amino acids. Alternatively, 20E could function as an autocrine signal that induces primary egg chambers to exit pre-vitellogenic arrest, while JH III could also activate the vitellogenic stage given its role in stimulating growth of primary egg chambers before pre-vitellogenic arrest (Hernández-Martínez et al., 2016; Zhao et al., 2016). We thus added each hormone to ex vivo ovary cultures in saline or Sf900 at physiological concentrations that were determined in prior studies (Brown et al., 2008; Gulia-Nuss et al., 2011; Dhara et al., 2013; Vogel et al., 2015). We then assessed EdU and anti-pHH3 labeling of follicle cells plus cytoophidia formation as indicators that a given treatment stimulated primary egg chambers to exit pre-vitellogenic arrest. No increase in EdU or pHH3 labeling occurred when ovaries were cultured in Sf900 or saline alone (Fig. 3A–D). Adding each hormone to saline also had no stimulatory effect (Fig. 3A and B). In contrast, ILP3 and OEH stimulated a significant increase in the number of EdU labeled follicle cells when ovaries were cultured in Sf900, whereas 20E and JH III did not (Fig. 3A–H). Adding ILP3 to Sf900 also strongly increased the number of follicle cells that were labeled by anti-pHH3 (Fig. 3B). Adding OEH, 20E and JH III all slightly but significantly increased the number of follicle cells that were labeled by anti-pHH3 when compared to ovaries in Sf900 alone (Fig. 3B). However, this increase was small relative to the increase that was induced by ILP3. Confocal microscopy showed that adding ILP3 or OEH to ovaries in Sf900 also stimulated cytoophidia formation in follicle cells of primary egg chambers (Fig. 3I-L) while no cytoophidia were ever observed when ovaries were cultured in saline or Sf900 alone or when 20E or JH III were added to ex vivo cultures in saline or Sf900.

### 3.3. ILP3 and OEH signaling inactivate GSK3 and induce max accumulation

ILPs are broadly conserved activators of the IIS pathway in insects and other animals, whereas *A. aegypti* and other mosquitoes are unusual in that the IIS pathway is activated by both ILPs and OEH (Brown et al., 2008; Wen et al., 2010; Gulia-Nuss et al., 2011; Vogel et al., 2015). A highly conserved indicator of IIS pathway activation in *A. aegypti* and other species is phosphorylation of Akt (pAkt), which phosphorylates several substrates with potential functions in oogenesis (Fig. 4A). These include GSK3 and the transcription factor Forkhead Box O (FoxO) that are inhibited when phosphorylated by pAkt, plus targets that are activated when phosphorylated by pAkt that lead to activation of TOR signaling that phosphorylates p70 S6 kinase (pS6K) (Laplante and Sabatini, 2013; Hansen et al., 2014; Valzania et al., 2018). Other signaling molecules linked to the IIS pathway include adenosine monophosphate-activated kinase (AMPK), which functions as a stress-activated energy sensor, and multiple mitogen-activated protein kinases (MAPKs) that include ERK, JNK, and p38 (Hansen et al., 2007; Sim and Denlinger, 2013; Das and Arur, 2017; Valzania et al., 2018). We therefore assessed the timing of IIS and TOR pathway activation in ovaries by monitoring the phosphorylation status of Akt and S6K on

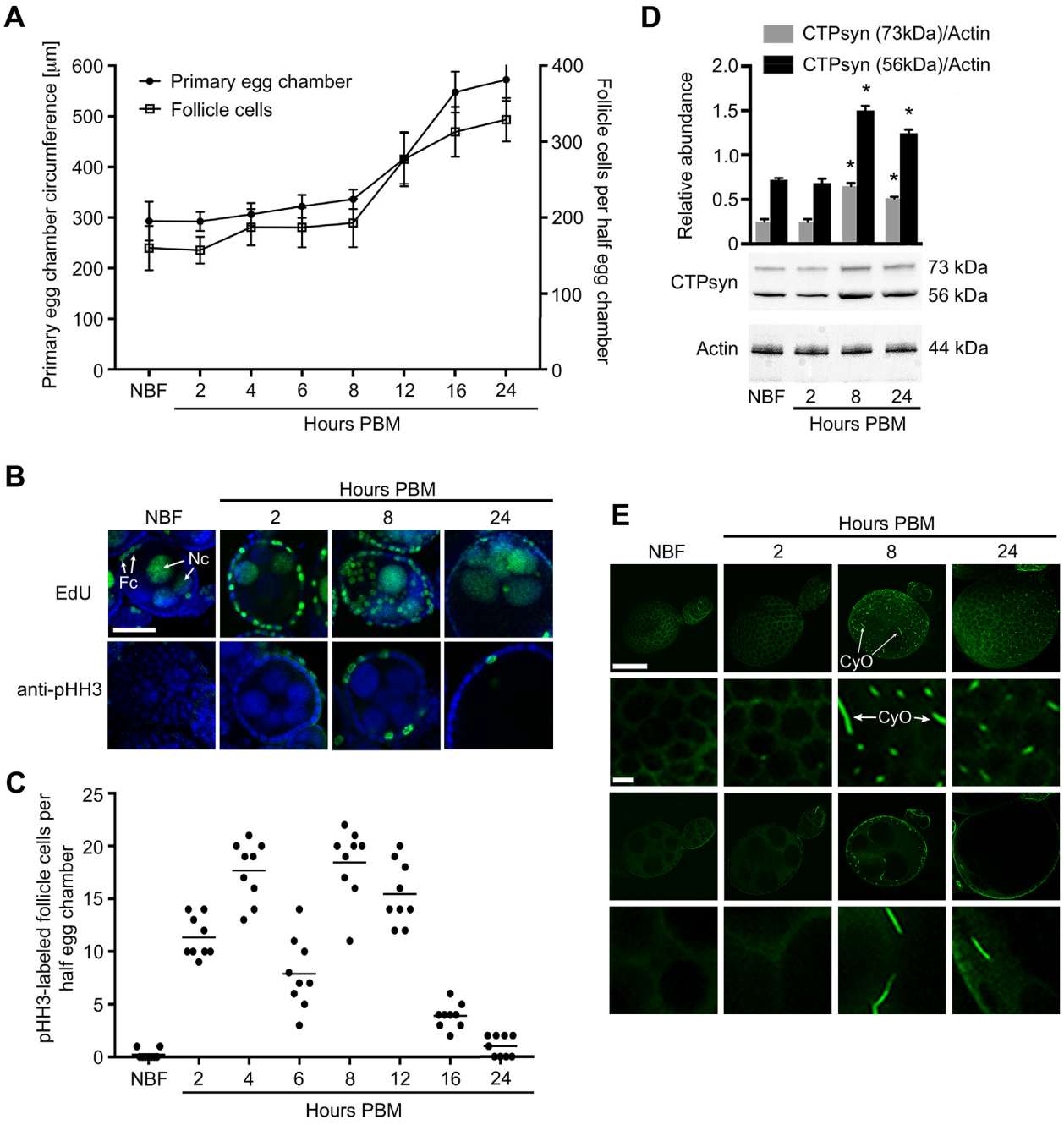


**Fig. 2.** Primary egg chambers exit pre-vitellogenic arrest by 8 h post-blood meal (PBM). (A) Mean circumference of primary egg chambers and mean number of follicle cells per half chamber (±standard deviation) in non-blood fed females (NBF) and 2–24 h PBM females. Three primary egg chambers from three ovary pairs were analyzed per time point. (B) Confocal images of primary egg chambers from NBF and 2–24 h PBM females after labeling with EdU (upper panel) or a phospho-histone H3 antibody (pHH3) (lower panel). EdU and pHH3 nuclei are green while unlabeled nuclei are blue after counterstaining with Hoechst 33342. Nc: nurse cells, Fc: follicle cells. Scale bar = 50 µm. (C) Number of pHH3 labeled follicle cells per half egg chamber from NBF and 2–24 h PBM females. Three primary egg chambers from three ovary pairs were measured per time point. Horizontal lines for each time point indicate the mean. (D) Immunoblots of ovary extracts (50 µg protein/lane) from NBF and 2–24 h PBM females probed with anti-CTPsyn or actin antibodies. The graph above the immunoblots shows the mean abundance (±standard deviation) of the 73 and 56 kDa proteins recognized by anti-CTPsyn relative to actin (44 kDa) from three immunoblots that were prepared from triplicate biological samples that were independently collected. Asterisks (*) above bars indicate that the 8 and 24 h PBM samples significantly differed from the NBF samples (ANOVA followed by post-hoc Dunnett's tests, $P < 0.0001$). (E) Confocal images of primary egg chambers from NBF and PBM females after labeling with anti-CTPsyn. First row: low magnification images of follicle cells showing cytoophidia (CyO) in the cytoplasm visualized by anti-CTPsyn. Second row: high magnification images of the same optical sections. Third row: low magnification optical sections through the center of primary egg chambers showing the presence of cytoophidia in nurse cells. Fourth row: high magnification of the same sections. Panels in first and third rows are at the same magnification with the scale bar in the left most panel in row one = 50 µm. The panels in second and fourth rows are also at the same magnification with the scale bar in the left most panel of row two = 5 µm.

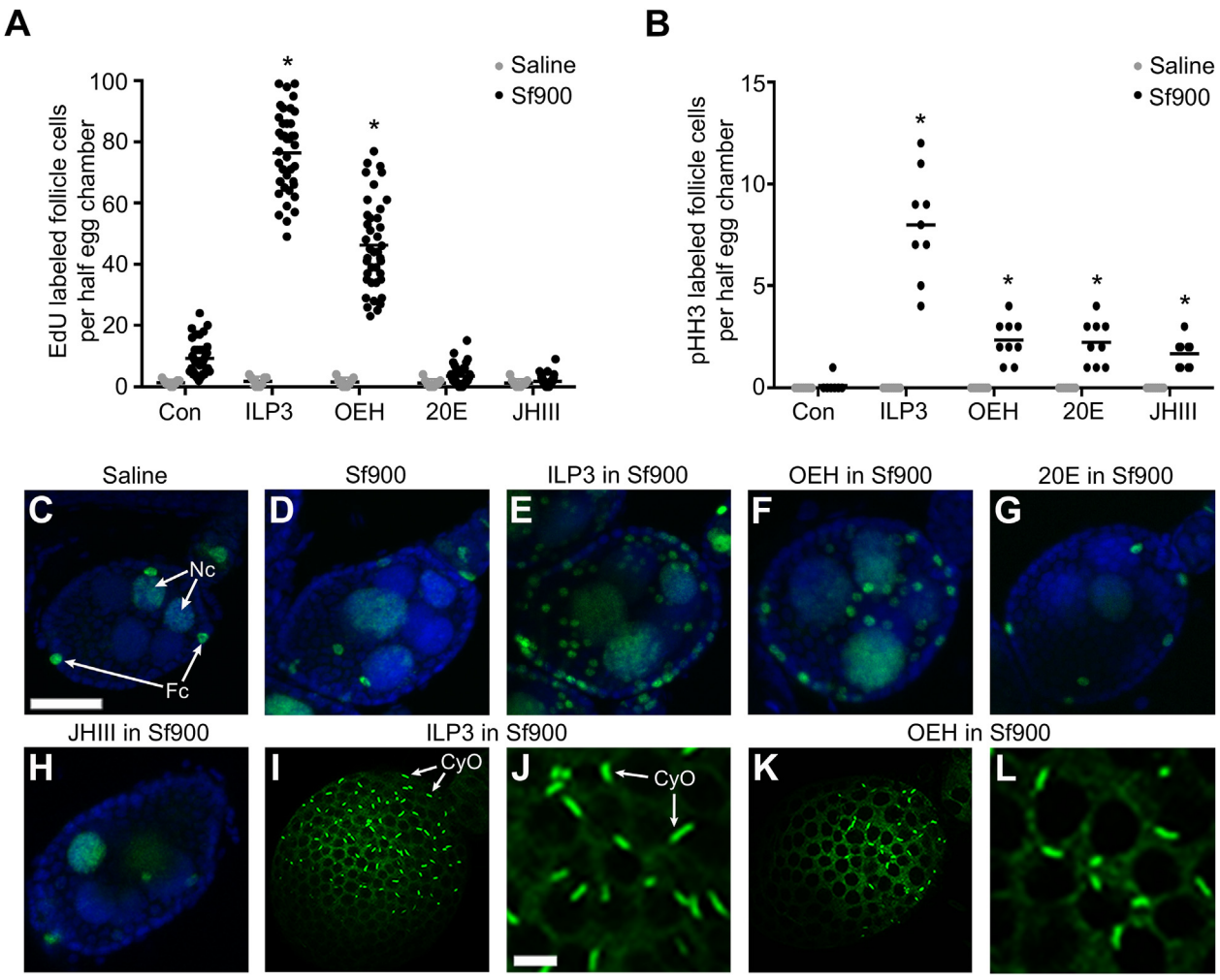


**Fig. 3.** ILP3 and OEH stimulate primary egg chambers to exit pre-vitellogenic arrest. (A) Number of follicle cells per half egg chamber (±standard deviation) that were EdU-labeled 6 h after ovaries from NBF females were placed in saline or Sf900 medium containing ILP3 (0.3 μM), OEH (0.3 μM), 20E (17 μM), or JH III (17 μM). Ovaries in saline or Sf900 alone (Con) served as the negative control. Four primary egg chambers from ten ovary pairs were analyzed per time point. Horizontal lines for treatment indicate the mean. Asterisks (*) above bars indicate treatments in Sf900 that were significantly higher than the negative control (ANOVA followed by a post-hoc Dunnett's test, $P < 0.001$). (B) Mean number of follicle cells per half chamber (±standard deviation) that were anti-pHH3 labeled 6 h after ovaries from NBF females were placed in saline or Sf900. Three primary egg chambers from a total of three ovary pairs were measured per time point. Horizontal lines for treatment indicate the mean. Asterisks (*) above bars indicate treatments that were significantly higher than the negative control (ANOVA followed by a post-hoc Dunnett's test, $P < 0.001$). (C–H) Confocal images showing EdU-labeled follicle (Fc) and nurse cell (Nc) nuclei (green) in primary egg chambers following select treatments from A and B. Note the much larger number of labeled follicle cells in E and F versus C and D. Unlabeled cell nuclei (blue) are stained with Hoechst 33342. Scale bar in C = 50 μm. (I–L) Confocal images showing cytoophidia (CyO) in follicle cells (Fc) visualized by anti-CTPsyn following select treatments from A and B. Scale bar in J = 5 μm.

immunoblots in concert with the phosphorylation status of GSK3, FoxO, AMPK and the aforementioned MAPKs. We also assessed the abundance of Max given evidence from other species for regulation of Myc/Max transcription factors by GSK3, and associated roles for Myc/Max in cell growth and cytoophidia formation (Parisi et al., 2011; Mauer et al., 2014; Gabay et al., 2014; Grifoni and Bellosta, 2015; Aughey et al. 2016). For ovaries collected directly from females, we detected little or no pAkt, pS6K, pGS3K or Max in ovaries from NBF females, whereas the abundance of each of these phosphorylated proteins increased 2–8 h PBM before declining at 24 h PBM (Fig. 4B). In contrast, ovaries from NBF and PBM females exhibited no differences in the phosphorylation status of FoxO, AMPK, ERK, JNK or p38 which were similarly abundant (Fig. S3).

In our ex vivo assay, pAkt, pS6K, pGS3K and Max were absent or only weakly detected in ovaries that were collected from NBF females and cultured in saline alone or saline plus OEH or ILP3 (Fig. 4C). The phosphorylated form of each protein was also absent or weakly detected in ovaries cultured in Sf900, whereas each strongly increased in abundance 30 min post-treatment with OEH or ILP3 and remained elevated at 6 h (Fig. 4D). In contrast, no differences were detected in the phosphorylation status of FoxO, AMPK, ERK, JNK or p38 before and after treating ovaries with OEH or ILP3 cultured in saline or Sf900 for 6 h (Fig. S3). Altogether, these findings indicated that ILP3 and OEH stimulated primary egg chambers to exit previtellogenic arrest, which further correlated with activation of the IIS and TOR pathways, phosphorylation of GSK3, and accumulation of Max.

### 3.4. *Exit from pre-vitellogenic arrest requires activation of the IIS and TOR pathways*

We added Torin 2, a second-generation inhibitor of TORC1 and TORC2 in vertebrates (Thoreen et al., 2009; Liu et al., 2013), to ex vivo ovary cultures in Sf900 to assess whether primary egg chambers require TOR signaling to exit pre-vitellogenic arrest. Since Torin 2 had not previously been used in *A. aegypti* or other insects, we first conducted

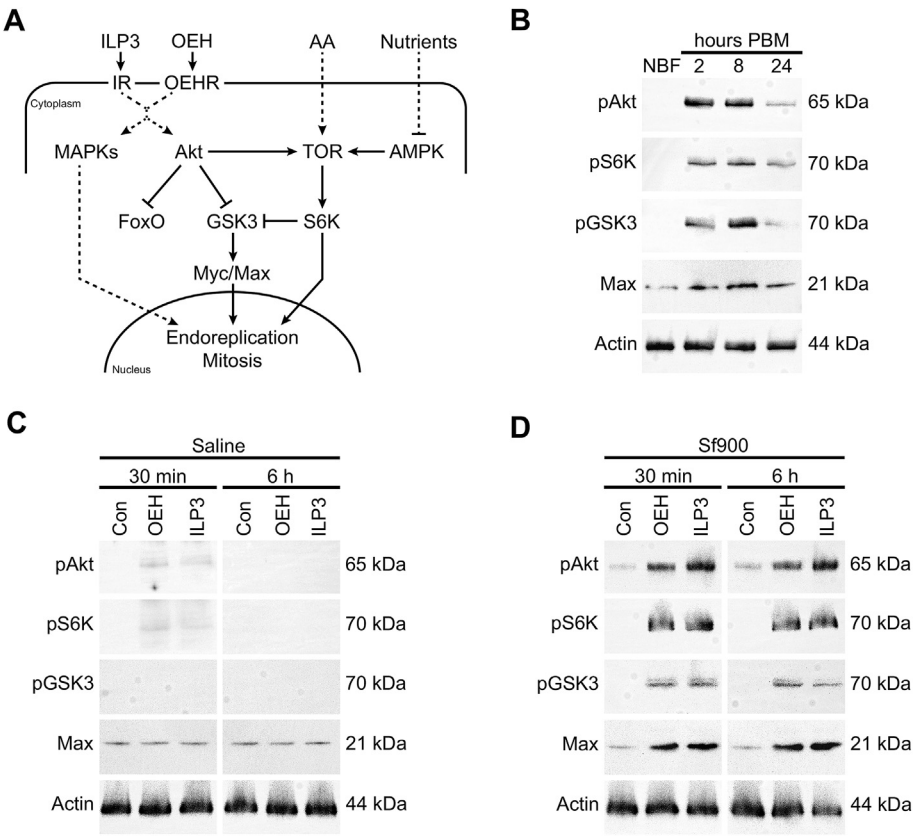


**Fig. 4.** Blood feeding, ILP3 and OEH activate the IIS and TOR pathways in ovaries. (A) Schematic showing key components of the IIS and TOR pathways. (B) Immunoblots of ovary extracts (50 μg of protein per lane) from NBF and 2–24 h PBM females. Samples were probed with antibodies to phosphorylated Akt (pAkt), pS6K, pGSK3, Max, or actin (which served as a loading control). Molecular masses of each protein are shown to the right. (C) Immunoblots of ovary extracts (50 μg of protein per lane) from ex vivo assays conducted in saline. Ovaries from NBF females were incubated in saline (Con), saline plus OEH (0.3 μM), or saline plus ILP3 (0.3 μM) for 30 min or 6 h. Blots were then probed with the same antibodies as in (B). (D) Immunoblots of ovary extracts (50 μg of protein per lane) from ex vivo assays conducted in Sf900. Incubation conditions and antibodies used to probe blots were the same as in (C).

dose-response assays. Results showed that Torin 2 inhibited EdU labeling of follicle cells in response to ILP3 or OEH with an $IC_{50}$ value of 50 pM (Figs. S4A and B). This effect was readily visible by confocal microscopy where adding 17 nM Torin 2 to ex vivo ovary cultures in Sf900 plus OEH or ILP3 near fully inhibited EdU labeling of follicle cells and cytoophidia formation (Fig. 5A and B). Immunoblotting correspondingly showed that 17 nM Torin 2 inhibited the accumulation of pS6K, pGSK3 and Max in response to OEH or ILP3 stimulation but did not reduce the accumulation of pAkt, which fully supported inhibition of TOR but not the IIS pathway (Fig. 5C). We then assessed the effects of OSI-906, which is a second-generation inhibitor of the mammalian IR and insulin growth factor 1 receptor (IGFR1) (Mulvihill et al., 2009). Again, since OSI-906 had not previously been used in insects, we conducted dose-response assays. Results showed that OSI-906 dose-dependently inhibited EdU labeling of follicle cells in primary egg chambers with an $IC_{50}$ value of 1.33 nM when ovaries were stimulated with ILP3 but only weakly reduced labeling with an $IC_{50}$ value of 840 nM when ovaries were stimulated by OEH (Figs. S4C and D). Confocal microscopy showed that

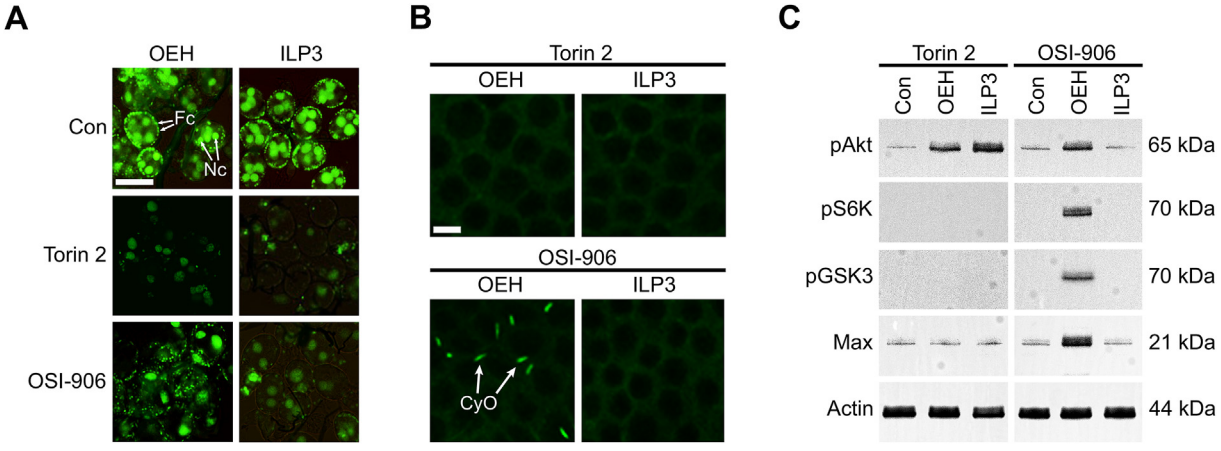


**Fig. 5.** Torin 2 inhibits TOR signaling while OSI-906 inhibits activation of the IIS pathway by ILP3. Ex vivo assays were conducted as in Fig. 4 by incubating ovaries from NBF females in Sf900 plus OEH or ILP3 (Con) or the same conditions plus Torin 2 (17 nM) or OSI-906 (170 nM). (A) Confocal images of primary egg chambers 6 h post-incubation showing the incorporation of EdU into follicle (Fc) and nurse cell (Nc) nuclei. Note that few follicle cells in the OEH and ILP3 treatments incorporate EdU in the presence of Torin 2 while several follicle cells are labeled in the OEH but not ILP3 treatment in the presence of OSI-906. (B) Confocal images of primary egg chambers 6 h post-incubation after labeling with anti-CTPsyn. No cytoophidia (CyO) are present in the OEH and ILP3 treatments in the presence of Torin 2, while numerous cytoophidia are visible in the OEH but not ILP3 treatment in the presence of OSI-906. (C) Immunoblots of ovary extracts (50 μg of protein per lane) probed with same antibodies as used in Fig. 4.

170 nM OSI-906 greatly reduced EdU labeling of follicle cells and fully inhibited cytoophidia formation when ovaries were stimulated with ILP3, but had no effect on these measures when ovaries were stimulated with OEH (Fig. 5A and B). Correspondingly, immunoblotting assays showed that 170 nM OSI-906 inhibited the accumulation of pAkt, pS6K, pGSK3 and Max when ovaries were stimulated with ILP3 but not OEH (Fig. 5C). We thus concluded that activation of the IIS and TOR pathways was essential for primary egg chambers to exit pre-vitellogenic arrest. These results also indicated that OSI-906 strongly inhibited activation of the IIS pathway after binding of ILP3 to the *A. aegypti* IR but at the same concentration did not inhibit activation of the IIS pathway after binding by OEH to the *A. aegypti* OEHR.

### 3.5. Direct inhibition of GSK3 stimulates primary egg chambers to exit pre-vitellogenic arrest

Since phosphorylation of GSK3 by pAkt inhibits its action (Zhang et al., 2006; Parisi et al. 2011), we examined whether direct inhibition of GSK3 also stimulates primary egg chambers to exit pre-vitellogenic arrest independently of activating the IIS and TOR pathways. This was approached by placing ovaries from NBF females in Sf900 plus CHIR-99021, which is a selective ATP competitive inhibitor of GSK3 (Ring et al., 2003; Bain et al., 2007; Kramer et al., 2012). CHIR-99021 induced a significant increase in the number of EdU-labeled follicle cell nuclei in primary egg chambers while also stimulating cytoophidia formation (Fig. 6A and B). Immunoblots of treated ovaries revealed that CHIR-99021 had no effect on phosphorylation of GSK3, which was induced by ILP3, but CHIR-99021 and ILP3 both stimulated an increase in the abundance of Max but not Myc (Fig. 6C). Since primary egg chambers only exited pre-vitellogenic arrest in response to ILP3 or OEH if ovaries were in Sf900, we further asked if CHIR-99021 could induce primary egg chambers to exit pre-vitellogenic arrest in the absence of increased nutrients. Strikingly, adding CHIR-99021 to ovaries in saline increased EdU-labeling of follicle cells, cytoophidia formation, and an increase in Max, whereas ILP3 failed to stimulate the phosphorylation of GSK3 or an increase in Max (Fig. 6D–F). These results strongly supported that primary egg chambers do not depend on the presence of amino acids or other nutrients to exit pre-vitellogenic arrest if GSK3 was directly inhibited.

## 4. Discussion

Yolk production and uptake by oocytes is an essential component of egg maturation by *A. aegypti* and other mosquitoes. Previous studies identified JH III, 20E, and the IIS/TOR pathways as key factors that regulate yolk protein expression by the fat body after a female blood feeds (Hansen et al., 2014; Roy et al., 2016), yet little was known prior to this study about the factors that maintain primary egg chambers in pre-vitellogenic arrest in the absence of blood feeding or that stimulate primary egg chambers to exit pre-vitellogenic arrest after a blood meal. Our ex vivo assays indicate that primary egg chambers exit pre-vitellogenic arrest in response to ILP3 and OEH but only if nutrients were also provided by culturing in Sf900 medium. Pharmacological interventions using Torin 2 and OSI-906 indicate that exit requires

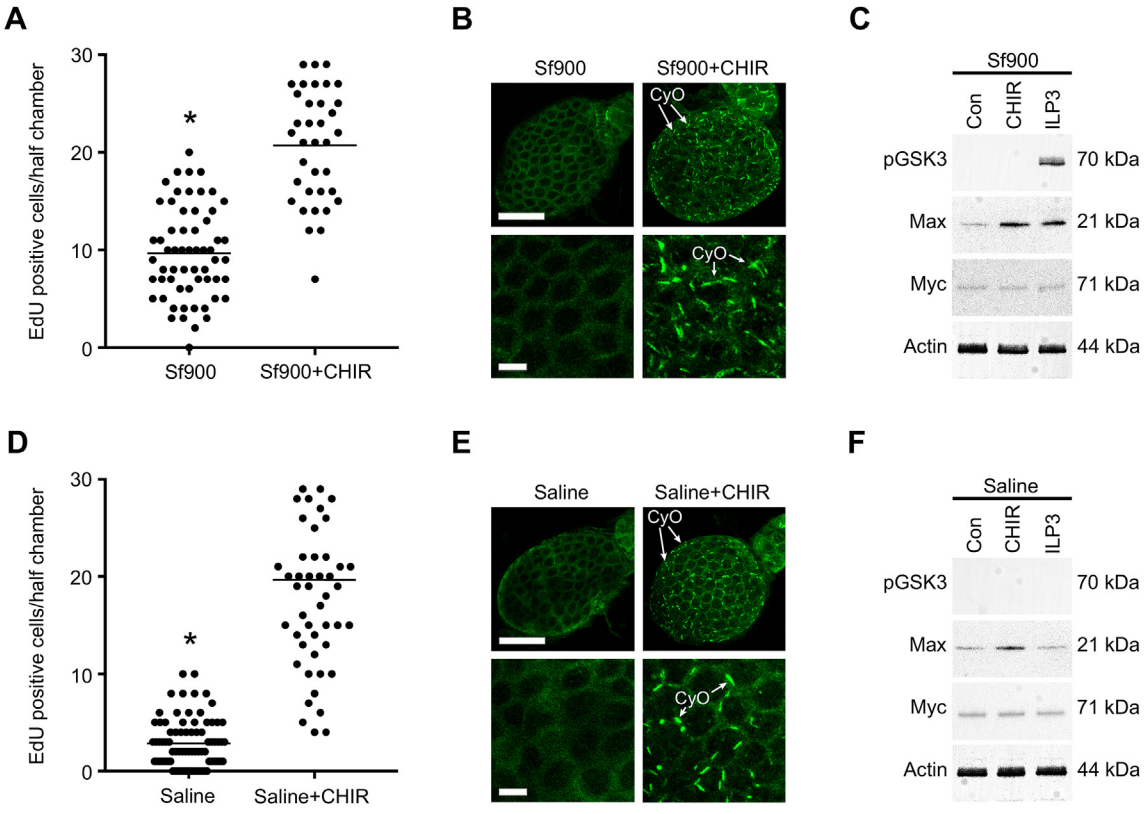


**Fig. 6.** The GSK3 inhibitor CHIR-99201 stimulates primary egg chambers to exit pre-vitellogenic arrest. Ex vivo assays were conducted as in Fig. 4 by incubating ovaries from NBF females in Sf900 or saline plus CHIR-99021 (200 μM) or ILP3 (0.3 μM) for 6 h. Ovaries in Sf900 or saline alone (Con) served as controls. (A–C) Outcomes of assays in Sf-900. (A) Number of follicle cell nuclei per half of a primary egg chamber that were labeled by EdU, (B) low (upper) and high (lower) magnification confocal images of cytoophidia (CyO) visualized in primary egg chambers by anti-CTPsyn, and (C) immunoblots of ovary extracts probed with anti-pGSK3, Max, Myc or actin. A total of sixty (Sf900) and thirty six primary egg chambers (Sf900 + CHIR) from ten ovary pairs were analyzed in (A) with the asterisk (*) indicating that significantly more EdU-labeled follicle cells were present in the CHIR-99201 treatment (*t*-test; $p < 0.001$). Horizontal lines in (A) indicate means. The scale bars in the upper and lower rows in (B) = 50 and 5 μm respectively, while the molecular masses of the proteins visualized in (C) are indicated to the right of each blot. (D–F) Outcomes of the same assays conducted in saline with asterisks (*), scale bars and protein masses defined as in (A–C).

activation of the IIS and TOR pathways, which correlates with inactivation of GSK3 via phosphorylation by pAkt and accumulation of Max. These findings thus overall suggest that maintenance of pre-vitellogenic arrest in NBF females requires active GSK3, while inactivation of GSK3 via ILP3/OEH release and pAkt mediated phosphorylation is a key factor in primary egg chambers exiting pre-vitellogenic arrest after a female blood feeds.

Our ex vivo assays indicate that primary egg chambers do not require an increase in nutrients as occurs after blood feeding to exit pre-vitellogenic arrest because direct inhibition of GSK3 by CHIR-99021 in PBS stimulated primary egg chambers to grow. Increased nutrients alone do not activate IIS/TOR signaling in ovaries, but ovaries do require increased nutrients for ILP3/OEH to activate the IIS and TOR pathways, which leads to inactivation of GSK3 via phosphorylation by pAkt. Sf900 is a commercially available medium that is used to maintain a number of established insect cell lines. Our results do not reveal the precise nutrients in Sf900 that ovaries require for responsiveness to OEH/ILP3 and associated activation of the IIS/TOR pathways. However, previous studies in *A. aegypti* and *D. melanogaster* indicate that amino acids are likely important since amino acid sensing in concert with ILPs activates TOR signaling in the fat body (Attardo et al., 2006; Parisi et al., 2011). However, this does not exclude the possibility that other nutrients could also play roles in OEH/ILP3 mediated activation of the IIS/TOR pathways in the ovaries. While results of this study identify redundant functions for ILP3 and OEH in activating primary egg chambers, previous data indicate that OEH more strongly stimulates follicle cells to produce 20E and other ecdysteroids than ILP3 (Brown et al., 2008; Wen et al., 2010). Reciprocally, while ILP3 plays a role in activating blood meal digestion by the midgut and yolk protein biosynthesis by the fat body, OEH has little or no effect on these functions (Gulia-Nuss et al., 2011). Thus, ILP3 and OEH only exhibit partially overlapping functional activities, which is due in part to the IR being broadly expressed in multiple organs including the ovaries, fat body and midgut, while the OEHR is preferentially expressed in follicle cells of primary egg chambers (Vogel et al., 2015). Because OEH and ILP3 bind different receptors, it is also possible that OEH and ILP3 exhibit currently unknown differences in downstream signaling activities that could also contribute to non-redundant functions during female reproduction.

Results of this study also highlight differences in how the IIS pathway regulates processes with essential functions in the vitellogenic stage of oogenesis in *A. aegypti*. For example, yolk protein expression by the fat body requires inactivation of FoxO via pAkt and co-stimulation with 20E (Roy et al., 2007; Hansen et al., 2007), whereas results from this study indicate that primary egg chambers require inactivation of GSK3 by pAkt to exit pre-vitellogenic arrest with no co-dependence on 20E, although ILP3 and OEH stimulate follicle cells to produce 20E (Brown et al., 2008). Our results do not identify any change in the abundance of pFoxO and FoxO in ovaries before or after blood feeding or in response to ILP3 and OEH in ex vivo assays. However, these data do not definitively indicate that inactivation of FoxO plays no role in oogenesis given studies in *D. melanogaster* implicating FoxO activation in arresting oogenesis during starvation (LaFever et al., 2010; Jouandin et al., 2014). Activation of the IIS and TOR pathways also overrides inhibition by FoxO3, which enables follicles to form oocytes in mammals (Zhang and Liu, 2015). While the IIS pathway can cross-signal through multiple MAPK pathways (Zhang and Liu, 2002; Zarubin and Han, 2005; Boucher et al., 2016; Teng et al., 2016), our results identified no alterations in the phosphorylation status of ERK, JNK or p38 in ovaries after blood feeding or treatment with ILP3 or OEH.

GSK3 has been implicated in regulating a range of cell survival, proliferation and growth processes in animals (Huang et al., 2009; Parisi et al., 2011; Mauer et al., 2014; Armstrong and Drummond-Barbosa, 2018). A number of predicted GSK3 substrates have also been identified including Myc family members that share basic helix-loop-helix zipper domains with Max and Mnt transcription factors. Myc dimerizes with Max and binds to promoter sites of several target genes to promote cell proliferation and growth but is inhibitory as a dimer with Mnt (Gregory et al., 2003; Pirity et al., 2006; Marandel et al., 2012; Gallant et al., 2013; Johnson et al., 2014; Gabay et al., 2014; Grifoni and Bellosta, 2015; Connacci-Sorrell et al., 2014; Gerlach et al., 2017). Myc protein accumulates in *D. melanogaster* S2 cells in response to activating the IIS and TOR pathways as well as in response to directly inhibiting GSK3 using lithium chloride (Parisi et al., 2011). This finding is consistent with results in other study systems which provide evidence that GSK3-mediated phosphorylation earmarks Myc for ubiquitylation and degradation, while inactivation of GSK3 promotes Myc persistence (Mauer et al., 2014; Hermida et al., 2017). Myc/Max dimerization has also been implicated in regulating cytoophidia formation in *D. melanogaster* egg chambers during oogenesis (Aughey et al., 2016). We similarly observe that inactivation of GSK3 promotes DNA replication in follicle cells and cytoophidia formation in the primary egg chambers of *A. aegypti* ovaries, but these responses correlate with the accumulation of Max rather than Myc. We thus speculate that Max may be the primary target for GSK3-mediated regulation of Myc/Max dimerization in the mosquito ovary. We also note that a small number of mosquitoes including *Aedes atropalpus* have evolved to produce eggs in the absence of blood feeding. However, our own previous studies indicate that blood meal independent release of ILPs and OEH from brain neurosecretory cells after eclosion is essential for *A. atropalplus* to produce mature eggs (Gulia-Nuss et al., 2012). Thus, the Akt/GSK3 branch of the IIS/TOR signaling pathway may similarly induce primary egg chambers to enter the vitellogenic stage in *A. atropalpus* by inactivating GSK3.

As previously noted, Torin 2 is a potent, selective inhibitor of TOR signaling in mammalian cells, while OSI-906 inhibits ligand binding-induced phosphorylation of the mammalian insulin and IGF1 receptors (Liu et al., 2013; Mulvihill et al., 2009). Results from this study show that Torin 2 strongly inhibits TOR signaling in *A. aegypti* ovaries in response to either ILP3 or OEH ($IC_{50} = 50$ pM), whereas OSI-906 much more strongly inhibits the *A. aegypti* IR ($IC_{50} = 1.33$ nM) than OEHR ($IC_{50} = 840$ nM). We also note that the $IC_{50}$ values for Torin 2 and OSI-906 in our follicle cell proliferation assays are lower than the $IC_{50}$ values calculated in proliferation/viability assays using mammalian cell lines (Zinn et al., 2013; Simioni et al., 2014), while exhibiting 50–100x greater activity than rapamycin and the IR inhibitor PQIP that have been previously used in studies with *A. aegypti* (Dhara et al., 2013; Valzania et al., 2018). While lithium chloride inhibits GSK3 in *D. melanogaster* (Sofola et al., 2010; Parisi et al., 2011), we detected no inhibition of GSK3 in *A. aegypti* in background studies. This led to our using CHIR-99021, which inhibited *A. aegypti* GSK3 at a similar concentration to studies conducted with some mammalian cell types (Wang et al., 2016) but a higher concentration used in others (Ring et al., 2003). Thus, our results overall indicate that Torin 2, OSI-906, and CHIR-99021 function as selective inhibitors of TOR, IR and GSK3 respectively in *A. aegypti*.

## 5. Conclusion

Results of this study advance understanding of oogenesis in *A. aegypti* by identifying the Akt/GSK3 branch of the IIS/TOR signaling pathway in regulating the transition from the pre-to the vitellogenic stage of oogenesis after a female blood feeds. Since mosquitoes are monophyletic and blood feeding is required for most species to produce eggs, we hypothesize that inactivation of GSK3 functions as a conserved switch that enables primary egg chambers to rapidly enter the vitellogenic stage of oogenesis in response to blood meal induced release of ILPs and OEH. Determining whether Max is a GSK3 substrate in *A. aegypti* and other mosquito species is one area of need for future study. Another is to better understand how inter-organ communication (Droujinine and Perrimon, 2016) and signaling through the IIS and TOR pathways differentially affect the midgut where blood meal digestion occurs, the fat body where yolk components are synthesized, and the ovaries where oogenesis occurs.

**Acknowledgements:**

We thank J. A. Johnson for management of the *A. aegypti* colony and our laboratories. This work was funded by a grant from the National Institutes of Health (RO1AI033108) to MRB and MRS, and the Georgia Agricultural Experiment Station.

## Appendix A. Supplementary data

Supplementary data to this article can be found online at https://doi.org/10.1016/j.ydbio.2019.05.011.

## References

Armstrong, A.R., Drummond-Barbosa, D., 2018. Insulin signaling acts in adult adipocytes via GSK-3β and independently of FOXO to control Drosophila female germline stem cell numbers. Dev. Biol. 440, 31–39.
Attardo, G.M., Hansen, I.A., Shiao, S.-H., Raikhel, A.S., 2006. Identification of two cationic amino acid transporters required for nutritional signaling during mosquito reproduction. J. Exp. Biol. 209, 3071–3078.
Aughey, G.N., Grice, S.J., Liu, J.L., 2016. The interplay between Myc and CTP synthase in *Drosophila*. PLoS Genet. 12, e1005867.
Bain, J., Plater, L., Elliott, M., Shapiro, N., Hastie, C.J., McLauchlan, H., Klevernic, I., Arthur, J.S., Alessi, D.R., Cohen, P., 2007. The selectivity of protein kinase inhibitors: a further update. Biochem. J. 408, 297–315.
Bastock, R., St Johnston, D., 2008. *Drosophila* oogenesis. Curr. Biol. 18, R1082–R1087.
Boucher, J., Softic, S., El Ouaamari, A., Krumpoch, M.T., Kleinridders, A., Kulkarni, R.N., O'Neill, B.T., Kahn, C.R., 2016. Differential roles of insulin and IGF-1 receptors in adipose tissue development and function. Diabetes 65, 2201–2213.
Brown, M.R., Graf, R., Swiderek, K.M., Fendley, D., Stracker, T.H., Champagne, D.E., Lea, A.O., 1998. Identification of a steroidogenic neurohormone in female mosquitoes. J. Biol. Chem. 273, 3967–3971.
Brown, M.R., Clark, K.D., Gulia, M., Zhao, Z., Garczynski, S.F., Crim, J.W., Suderman, R.J., Strand, M.R., 2008. An insulin-like peptide regulates egg maturation and metabolism in the mosquito *Aedes aegypti*. Proc. Natl. Acad. Sci. U.S.A. 105, 5716–5721.
Burn, K.M., Shimada, Y., Ayers, K., Lu, F., Hudson, A.M., Cooley, L., 2015. Somatic insulin signaling regulates a germline starvation response in *Drosophila* egg chambers. Dev. Biol. 398, 206–217.
Clarke, I.J., Arbabi, L., 2016. New concepts of the central control of reproduction, integrating influence of stress, metabolic state, and season. Domest. Anim. Endocrinol. 56 (Suppl. l), S165–S179.
Clements, A., 1992. The Biology of Mosquitoes. Chapman & Hall, London.
Connacci-Sorrell, M., McFerrin, L., Eisenman, R.N., 2014. An overview of MYC and its interactome. Cold Spring Harb. Perspect. Med. 1, a014357.
Das, D., Arur, S., 2017. Conserved insulin signaling in the regulation of oocyte growth, development, and maturation. Mol. Reprod. Dev. 84, 444–459.
Dhara, A., Eum, J.-H., Robertson, A., Gulia-Nuss, M., Vogel, K.J., Clark, K.D., Graf, R., Brown, M.R., Strand, M.R., 2013. Ovary ecdysteroidogenic hormone functions independently of the insulin receptor in the yellow fever mosquito, *Aedes aegypti*. Insect Biochem. Mol. Biol. 43, 1100–1108.
Droujinine, I.A., Perrimon, N., 2016. Interorgan communication pathways in physiology: focus on *Drosophila*. Annu. Rev. Genet. 50, 539–570.
Drummond-Barbosa, D., Spradling, A.C., 2001. Stem cells and their progeny respond to nutritional changes during *Drosophila* oogenesis. Dev. Biol. 231, 265–278.
Gabay, M., Li, Y., Felsher, D.W., 2014. MYC activation is a hallmark of cancer initiation and maintenance. Cold Spring Harbor Perspect. Med. 4, a014241.
Gallant, P., 2013. Myc function in *Drosophila*. Cold Spring Harbor Perspect. Med. 3, a014324.
Gancz, D., Gilboa, L., 2013. Insulin and target of rapamycin signaling orchestrate the development of ovarian niche-stem cell units in *Drosophila*. Development 140, 4145–4154.
Gerlach, J.M., Furrer, M., Gallant, M., Birkel, D., Balupuri, A., Wolf, E., Gallant, P., 2017. PAF1 complex component Leo 1 helps recruit *Drosophila* Myc to promoters. Proc. Natl. Acad. Sci. U.S.A. 114, E9224–E9232.
Gregory, M.A., Qi, Y., Hann, S.R., 2003. Phosphorylation by glycogen synthase kinase-3 controls c-myc proteolysis and subnuclear localization. J. Biol. Chem. 278, 51606–51612.
Grifoni, D., Bellosta, P., 2015. *Drosophila* Myc: a master regulator of cellular performance. Biochim. Biophys. Acta 1849, 570–581.
Gu, L., Liu, H., Gu, X., Boots, C., Moley, K.H., Wang, Q., 2015. Metabolic control of oocyte development: linking maternal nutrition and reproductive outcomes. Cell. Mol. Life Sci. 72, 251–271.
Gulia-Nuss, M., Robertson, A.E., Brown, M.R., Strand, M.R., 2011. Insulin-like peptides and the target of rapamycin pathway coordinately regulate blood digestion and egg maturation in the mosquito *Aedes aegypti*. PLoS One 6, e20401.
Gulia-Nuss, M., Eum, J.H., Strand, M.R., Brown, M.R., 2012. Ovary ecdysteroidogenic hormone activates egg maturation in the mosquito *Georgecraigius atropalpus* after adult eclosion or a blood meal. J. Exp. Biol. 215, 3758–3767.
Gulia-Nuss, M., Elliot, A., Brown, M.R., Strand, M.R., 2015. Multiple factors contribute to anautogenous reproduction by the mosquito *Aedes aegypti*. J. Insect Physiol. 82, 8–16.
Gwadz, R.W., Spielman, A., 1973. Corpus allatum control of ovarian development in *Aedes aegypti*. J. Insect Physiol. 19, 1441–1448.
Hagedorn, H.H., Turner, S., Hagedorn, E.A., Pontecorvo, D., Greenbaum, P., Pfeiffer, D., Wheelock, G., Flanagan, T.R., 1977. Postemergence growth of the ovarian follicles of *Aedes aegypti*. J. Insect Physiol. 23, 203–206.
Hansen, I.A., Sieglaff, D.H., Munro, J.B., Shiao, S.H., Cruz, J., Lee, I.W., Heraty, J.M., Raikhel, A.S., 2007. Forkhead transcription factors regulate mosquito reproduction. Insect Biochem. Mol. Biol. 37, 985–997.
Hansen, I.A., Attardo, G.M., Rodriguez, S.D., Drake, L.L., 2014. Four-way regulation of mosquito yolk protein precursor genes by juvenile hormone-, ecdysone-, nutrient-, and insulin-like peptide signaling pathways. Front. Physiol. 5, 103.
Hartman, T.R., Strochlic, T.I., Ji, Y., Zinshteyn, D., O'Reilly, A.M., 2013. Diet controls *Drosophila* follicle stem cell proliferation via Hedgehog sequestration and release. J. Cell Biol. 201, 741–757.
Hermida, M.A., Dinesh Kumar, J., Leslie, N.R., 2017. GSK3 and its interactions with the PI3K/AKT/mTOR signalling network. Adv. Biol. Regul. 65, 5–15.
Hernández-Martínez, S., Mayoral, J.G., Li, Y., Noriega, F.G., 2007. Role of juvenile hormone and allatotropin on nutrient allocation, ovarian development and survivorship in mosquitoes. J. Insect Physiol. 53, 230–234.
Hernández-Martínez, S., Rivera-Perez, C., Nouzova, M., Noriega, F.G., 2016. Coordinated changes in JH biosynthesis and JH hemolymph titers in *Aedes aegypti* mosquitoes. J. Insect Physiol. 72, 22–27.
Huang, J., Zhang, Y., Bersenev, A., O'Brien, W.T., Tong, W., Emerson, S.G., Klein, P.S., 2009. Pivotal role for glycogen synthase kinase-3 in hematopoietic stem cell homeostasis in mice. J. Clin. Investig. 119, 3519–3529.
Huang, J., Kalderon, D., 2014. Coupling of Hedgehog and Hippo pathways promotes stem cell maintenance by stimulating proliferation. J. Cell Biol. 205, 325–338.
Ikegami, K., Yoshimura, T., 2016. Comparative analysis reveals the underlying mechanism of vertebrate seasonal reproduction. Gen. Comp. Endocrinol. 227, 64–68.
Johnson, D.W., Llop, J.R., Farrell, S.F., Yuan, J., Stolzenburg, L.R., Samuelson, A.V., 2014. The *Caenorhabditis elegans* Myc-Mondo/Mad complexes integrate diverse longevity signals. PLoS Genet. 10, e1004278.
Jouandin, P., Ghiglione, C., Noselli, S., 2014. Starvation induces FoxO-dependent mitotic-to-endocycle switch pausing during *Drosophila* oogenesis. Development 141, 3013–3021.
Kramer, T., Schmidt, B., Lo Monte, F., 2012. Small-molecule inhibitors of GSK-3: structural insights and their application to Alzheimer's disease models. Int. J. Alzheimer's Dis. 2012, 381029.
LaFever, L., Drummond-Barbosa, D., 2005. Direct control of germline stem cell division and cyst growth by neural insulin in *Drosophila*. Science 309, 1071–1073.
LaFever, L., Feoktistov, A., Hsu, H.J., Drummond-Barbosa, D., 2010. Specific roles of target of rapamycin in the control of stem cells and their progeny in the *Drosophila* ovary. Development 137, 2117–2126.
Laplante, M., Sabatini, D.M., 2013. Regulation of mTORC1 and its impact on gene expression at a glance. J. Cell Sci. 126, 1713–1719.
Laurence, B.R., 1977. Ovary development in mosquitoes: a review. Adv. Invert. Repro. 1, 154–165.
Laurence, B., Simpson, M., 1974. Cell replication in the follicular epithelium of the adult mosquito. J. Insect Physiol. 20, 703–715.
Laws, K.M., Drummond-Barbosa, D., 2016. AMP-activated protein kinase has diet-dependent and -independent roles in *Drosophila* oogenesis. Dev. Biol. 420, 90–99.
Lee, K.W., 2015. Dietary protein: carbohydrate balance is a critical modulator of lifespan and reproduction in *Drosophila melanogaster*: a test using a chemically defined diet. J. Insect Physiol. 75, 12–19.
Liu, J.-L., 2010. Intracellular compartmentation of CTP synthase in *Drosophila*. J. Genet. Genomics 37, 281–296.
Liu, J.-L., 2016. The cytoophidium and its kind: filamentation and compartmentation of metabolic enzymes. Annu. Rev. Cell Dev. Biol. 32, 349–372.
Liu, Q., Xu, C., Kirubakaran, S., Zhang, X., Hur, W., Liu, Y., Kwiatkowski, N.P., Wang, J., Westover, K.D., Gao, P., et al., 2013. Characterization of Torin2, an ATP-competitive inhibitor of mTOR, ATM, and ATR. Cancer Res. 73, 2574–2586.
Lucy, M.C., 2011. Growth hormone regulation of follicular growth. Reprod. Fertil. Dev. 24, 19–28.
Mauer, U., Preiss, F., Brauns-Schubert, P., Schlicher, L., Charvet, C., 2014. GSK-3 at the crossroads of cell death and survival. J. Cell Sci. 127, 1369–1378.
Marandel, L., Labbe, C., Bobe, J., Le Bail, P.Y., 2012. Evolutionary history of c-myc in teleosts and characterization of the duplicated c-myca genes in goldfish embryos. Mol. Reprod. Dev. 79, 85–96.
Meiselman, M., Lee, S.S., Tran, R.T., Dai, H., Ding, Y., Rivera-Perez, C., Wijesekera, T.P., Dauwalder, B., Noriega, F.G., Adams, M.E., 2017. Endocrine network essential for reproductive success in *Drosophila melanogaster*. Proc. Natl. Acad. Sci. U.S.A. 114, E3849–E3858.
Mulvihill, M.J., Cooke, A., Rosenfeld-Franklin, M., Buck, E., Foreman, K., Landfair, D., O'Connor, M., Pirritt, C., Sun, Y., Yao, Y., Arnold, L.D., Gibson, N.W., Ji, Q.S., 2009. Discovery of OSI-906: a selective and orally efficacious dual inhibitor of the IGF-1 receptor and insulin receptor. Future Med. Chem. 1, 1153–11571.
Parisi, F., Riccardo, S., Daniel, M., Saqcena, M., Kundu, N., Pession, A., Grifoni, D., Stocker, H., Tabak, E., Bellosta, P., 2011. *Drosophila* insulin and target of rapamycin (TOR) pathways regulate GSK3 beta activity to control Myc stability and determine Myc expression in vivo. BMC Biol. 9, 65.
Park, T.S., O'Brien, D.J., Carman, G.M., 2003. Phosphorylation of CTP synthetase on Ser 36, Ser 330, Ser 354, and Ser 454 regulates levels of CTP and phosphatidylcholine synthesis in *Saccharomyces cerevisiae*. J. Biol. Chem. 278, 20785–20794.
Pirity, J., Blanck, K., Schreiber-Agus, N., 2006. Lessons learned from Myc/Max/Mad knockout mice. Curr. Top. Microbiol. Immunol. 302, 205–234.

Riehle, M.A., Brown, M.R., 2002. Insulin receptor expression during development and a reproductive cycle in the ovary of the mosquito *Aedes aegypti*. Cell Tissue Res. 308, 409–420.
Ring, D.B., Johnson, K.W., Henriksen, E.J., Nuss, J.M., Goff, D., Kinnick, T.R., Ma, S.T., Reeder, J.W., Samuels, I., Slabiak, T., Wagman, A.S., Hammond, M.E., Harrison, S.D., 2003. Selective glycogen synthase kinase 3 inhibitors potentiate insulin activation of glucose transport and utilization in vitro and in vivo. Diabetes 52, 588–595.
Roy, S.G., Hansen, I.A., Raikhel, A.S., 2007. Effect of insulin and 20-hydroxyecdysone in the fat body of the yellow fever mosquito, *Aedes aegypti*. Insect Biochem. Mol. Biol. 37, 1317–1326.
Roy, S., Saha, T.T., Johnson, L., Zhao, B., Ha, J., White, K.P., Girke, T., Zou, Z., Raikhel, A.S., 2015. Regulation of gene expression patterns in mosquito reproduction. PLoS Genet. 11, e1005450.
Roy, S., Smykal, V., Johnson, L., Saha, T.T., Zou, Z., Raikhel, A.S., 2016. Regulation of reproductive processes in female mosquitoes. Adv. Insect Physiol. 51, 115–144.
Sim, C., Denlinger, D., 2013. Juvenile hormone III suppresses forkhead of transcription factor in the fat body and reduces fat accumulation in the diapausing mosquito, *Culex pipiens*. Insect Mol. Biol. 22, 1–11.
Simioni, C., Cani, A., Martelli, A.M., Zauli, G., Tabellini, G., McCubrey, J., Capitani, S., Neri, L.M., 2014. Activity of the novel mTOR inhibitor Torin-2 in B-precursor acute lymphoblastic leukemia and its therapeutic potential to prevent Akt reactivation. Oncotarget 5, 10034–10047.
Sofola, O., Kerr, F., Rogers, I., Killick, R., Augustin, H., Gandy, C., Allen, M.J., Hardy, J., Lovestone, S., Partridge, L., 2010. Inhibition of GSK-3 ameliorates Abeta pathology in an adult-onset *Drosophila* model of Alzheimer's disease. PLoS Genet. 6, e1001087.
Strand, M.R., Brown, M.R., Vogel, K.J., 2016. Mosquito peptide hormones: diversity, production, and function. Adv. Insect Physiol. 51, 145–188.
Teng, J.-A., Wu, S.-G., Chen, J.-X., Qiang, L., Peng, F., Zhu, Z., Qin, J., He, Z.-Y., 2016. The activation of ERK1/2 and JNK MAPK signaling by insulin/IGF-1 is responsible for the development of colon cancer with type 2 diabetes mellitus. PLoS One 1, e0149822.
Thoreen, C.C., Kang, S.A., Chang, J.W., Liu, Q., Zhang, J., Gao, Y., Reichling, L.J., Sim, T., Sabatini, D.M., Gray, N.S., 2009. An ATP-competitive mammalian target of rapamycin inhibitor reveals rapamycin-resistant functions of mTORC1. J. Biol. Chem. 284, 8023–8032.
Valzania, L., Coon, K.L., Vogel, K.J., Brown, M.R., Strand, M.R., 2018. Hypoxia-induced transcription factor signaling is essential for larval growth of the mosquito *Aedes aegypti*. Proc. Natl. Acad. Sci. U.S.A. 115, 457–465.
Vogel, K.J., Brown, M.R., Strand, M.R., 2015. Ovary ecdysteroidogenic hormone requires a receptor tyrosine kinase to activate egg formation in the mosquito *Aedes aegypti*. Proc. Natl. Acad. Sci. U.S.A. 112, 5057–5062.
Wang, S., Ye, L., Li, M., Liu, J., Jiang, C., Hong, H., Zhu, H., Sun, Y., 2016. GSK-3β inhibitor CHIR-99021 promotes proliferation through upregulating β-catenin in neonatal atrial human cardiomyocytes. J. Cardiovasc. Pharmacol. 68, 425–432.
Wen, Z., Gulia, M., Clark, K.D., Dhara, A., Crim, J.W., Strand, M.R., Brown, M.R., 2010. Two insulin-like peptide family members from the mosquito *Aedes aegypti* exhibit differential biological and receptor binding activities. Mol. Cell. Endocrinol. 328, 47–55.
Zarubin, T., Han, J., 2005. Activation and signaling of the p38 MAP kinase pathway. Cell Res. 15, 11–18.
Zhang, W., Liu, H.T., 2002. MAPK signal pathways in the regulation of cell proliferation in mammalian cells. Cell Res. 12, 9–18.
Zhang, H.H., Lipovsky, A.I., Dibble, C.C., Sahin, M., Manning, B.D., 2006. S6K1 regulates GSK3 under conditions of mTOR-dependent feedback inhibition of Akt. Mol. Cell 24, 185–197.
Zhang, D.B., Wang, Y., Liu, A.K., Wang, X.H., Dang, C.W., Yao, Q., Chen, K.P., 2013. Phylogenetic analysis of vector mosquito basic helix loop helix transcription factors. Insect Mol. Biol. 22, 608–621.
Zhang, H., Liu, K., 2015. Cellular and molecular regulation of the activation of mammalian primordial follicles: somatic cells initiate follicle activation in adulthood. Hum. Reprod. Update 21, 779–786.
Zhao, B., Hou, Y., Wang, J., Kokoza, V.A., Saha, T.T., Wang, X.L., Lin, L., Zou, Z., Raikhel, A.S., 2016. Determination of juvenile hormone titers by means of LC-MS/MS/MS and a juvenile hormone-responsive Gal4/UAS system in *Aedes aegypti* mosquitoes. Insect Biochem. Mol. Biol. 77, 69–77.
Zhu, J., Noriega, F.G., 2016. The role of juvenile hormone in mosquito development and reproduction. Adv. Insect Physiol. 51, 93–113.
Zinn, R.L., Gardner, E.E., Marchionni, L., Murphy, S.C., Dobromilskaya, I., Hann, C.L., Rudin, C.M., 2013. ERK phosphorylation is predictive of resistance to IGF-1R inhibition in small cell lung cancer. Mol. Cancer Ther. 12, 1131–1139.